Sum-frequency generation of a laser and its background in an on-chip lithium-niobate microdisk

Zhenzhong Hao (郝振中)[1], Li Zhang (张 莉)[1], Jie Wang (王 杰)[1], Fang Bo (薄 方)[1,2*], Feng Gao (高 峰)[1,2], Guoquan Zhang (张国权)[1,2**], and Jingjun Xu (许京军)[1,2***]
[1] MOE Key Laboratory of Weak-Light Nonlinear Photonics, TEDA Institute of Applied Physics and School of Physics, Nankai University, Tianjin 300457, China
[2] Collaborative Innovation Center of Extreme Optics, Shanxi University, Taiyuan 030006, China

*Corresponding author: bofang@nankai.edu.cn
**Corresponding author: zhanggq@nankai.edu.cn
***Corresponding author: jjxu@nankai.edu.cn
Received May 15, 2022 | Accepted June 14, 2022 | Posted Online July 14, 2022

Lithium-niobate microcavities have not only the ability to resonantly enhance light-matter interaction but also excellent nonlinear optical properties, thereby providing an important platform for nonlinear optical investigations. In this paper, we report the observation of multi-peak spectra in the near infrared range in lithium-niobate microcavities on a chip under the pump of a 1550 nm continuous laser. Such a multi-peak spectrum was attributed to the sum-frequency of the pump laser and its background. The conversion efficiencies of the sum-frequency processes are of the order of 61.5% W^{-1}. The influences of the phenomenon on nonlinear processes were further discussed.

Keywords: lithium niobate; microcavities; nonlinear optics.
DOI: 10.3788/COL202220.111902

1. Introduction

Whispering gallery mode (WGM) microcavities have attracted much attention in recent years for their broad applications ranging from ultra-sensitive sensing[1], enhanced nonlinear optical effects[2,3] to tunable quantum light sources[4]. These applications benefit from the ability of WGM microcavities to confine light for a long time, which is indicated by quality (Q) factors, in a small mode volume (V) via total internal reflection. Such light trapping mechanisms make WGM microcavities have high Q in very broad spectrum ranges, which is only limited by the transparency window of the material of which the microcavities are made.

It is known that putting a nonlinear optical medium into a high-Q optical cavitiy can improve the efficiencies of the nonlinear optical effects and release the requirement of high intensity pump. Therefore, a pulse laser with high peak power can be replaced by a continuous pump with power even lower than milliwatts. Compared with bulk optical cavities containing nonlinear optical materials, WGM microcavities usually have not only a much smaller size but also a broader resonance window in which high Q can be achieved[5,6]. Therefore, WGM microcavities made of nonlinear optical materials become an excellent testbed for nonlinear optical investigations. Various nonlinear optical effects[7,8] and their cascaded effects[9,10] were observed in high-Q WGM microcavities. Based on cascaded four-wave mixing[11] processes, optical frequency combs[12] that have great important applications in precision measurement are intensively investigated in high-Q WGM microcavities.

Lithium niobate (LN) is a noncentrosymmetrical material with outstanding nonlinear optical properties ($d_{33} = 27\,\mathrm{pm/V}$[13]). LN thin film on insulator has aroused wide interest and broad application prospects[14–16]. WGM microcavities made of LN take the advantages of LN and WGM cavities and therefore show great potential in fundamental studies and practical applications of second nonlinear optical effects such as second harmonic generation (SHG)[2,17–22], cascaded harmonic generation[23], sum-frequency generation (SFG)[24,25], and optical parametric oscillation[26–28]. Optical devices including entangled photon pairs[29] and optical frequency combs[30] were recently reported in LN WGM microcavities.

However, all of the nonlinear optical effects reported in LN WGM microcavities are associated with only laser sources. In this paper, we report the observation of a series of nonlinear optical signals, besides second harmonic signals, in an on-chip LN WGM microcavity. These nonlinear optical signals were attributed to the SFGs between the pump laser and its background. This work elucidates the origin of unknown nonlinear optical signals always observed in high-Q WGM resonators that cannot be attributed to high-order harmonic generation.

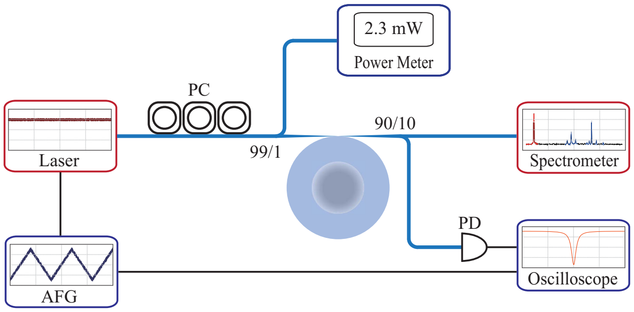

Fig. 1. Schematic of the experimental setup to measure sum-frequency signals. An arbitrary function generator (AFG) is used to precisely control the output wavelength of the pump laser and to trigger the oscilloscope. The pump light passes through a fiber polarization controller (PC) and a beam splitter, and then couples into the LN WGM microcavity via a tapered fiber. The transmission of the pump is monitored by a photodetector connected to an oscilloscope. The tapered fiber that is used to couple the pump collects the nonlinear optical signals as well. The nonlinear optical signals are detected by a spectrometer.

2. Samples and Experimental Setup

LN WGM microcavities with a size of 200 nm in thickness and 40 μm in radius were employed to conduct nonlinear optical experiments. The Q factors of these WGM microcavities are on the order of 10^5, which were fabricated from Z-cut LN film produced by NANOLN by using the microfabrication technique including UV lithography, argon ion etching, and hydrogen fluoride etching. For a Z-cut LN WGM microcavity, the optical axis of LN is parallel to the rotational axis of the microdisk cavity, in other words, perpendicular to the plane in which the microdisk lies.

Figure 1 indicates the experimental setup to observe the sum-frequency signal in the LN WGM microcavities. A tapered fiber was used to couple the 1550 nm pump into the LN microdisk and extract nonlinear optical signals from the same cavity. The 1550 nm pump is generated by a tunable laser with a linewidth less than 200 kHz and a tuning range covering 1520–1570 nm. The nonlinear optical signals were detected by a spectrometer allowing for the detection of weak light with power down to several picowatts (pW). The laser wavelength can be finely tuned by applying a triangular wave voltage on the piezo mirror of the external reference cavity of the laser. The transmission of the pump light was monitored by using a photodetector and an oscilloscope. An optical spectrum analyzer (not shown in Fig. 1) working from 600 nm to 1700 nm that covers the output wavelength of the pump laser was used to measure the transmission spectrum of the laser and its background and to calibrate the wavelengths measured by the spectrometer and shown by the laser controller. Therefore, we can approximately assign the WGMs related to the sum-frequency processes.

3. Experimental Results and Discussions

It is known that second-order nonlinear optical signals can be detected in WGM microcavities made from material lacking of central symmetry with pump down to less than milliwatts[20] when energy, angular momentum conversations, and multiple resonance are fulfilled simultaneously. When one pump was launched into an LN WGM, several kinds of nonlinear optical processes were reported: (1) optical parametric oscillation producing two photons with lower energy[27], (2) SHG giving rise to one photon with energy twice that of the pump[31], (3) sum-frequency between the pump and its second harmonic signal generating a third harmonic signal and other kinds of signals with even higher photon energy[32], and (4) Raman signal with wavelength longer than the pump[33].

We observed nonlinear optical signals with about 10 peaks, as shown in Fig. 2, when only one pump laser at 1521.36 nm was launched into an LN WGM microcavity. Peak 1, which is highlighted in red, has a wavelength of 760.68 nm. It is considered the second harmonic signal of the pump according to the principle of energy conservation, which indicated that the wavelength of the second harmonic signal was half of the pump wavelength. Besides the second harmonic signal, a series of signals ranging from 770 nm to 780 nm, marked in blue in Fig. 2, were unexpectedly observed as well. The nonlinear optical signals in blue have wavelengths between the pump at 1521.36 nm and its second harmonic signal of 760.68 nm, which is different from the aforementioned four kinds of nonlinear optical signals in the wavelength. Such nonlinear signals have not been discussed in detail in LN WGM cavities.

To find the origin of the unexpected nonlinear optical signals, we first suppose they are the sum-frequency signals of the pump and unknown light sources. In this situation, the wavelengths of the undiscovered light sources can be calculated according to energy conversation for sum-frequency processes, i.e., $hc/\lambda_{SFG} = hc/\lambda_P + hc/\lambda_{Cal}$, where h is the Planck constant; c is the light speed in vacuum; λ_{SFG} and λ_P are the wavelengths of the nonlinear signal and the pump, respectively; λ_{Cal} stands for the wavelength of the unknown light that is needed to mix with the pump to produce the SFG signal. The calculated wavelengths are shown in the third column of Table 1. On the other hand, the transmission spectrum of the pump laser was measured by an optical spectrum analyzer, which is shown in Fig. 3(a). Figure 3(b) is the enlarged version showing the detailed

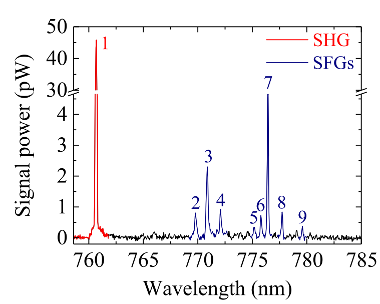

Fig. 2. Nonlinear optical signals. Peak 1, marked in red, corresponding to the second harmonic generation (SHG) of the pump laser at 1521.36 nm. Peaks 2–9 in blue are the sum-frequency generation (SFG) signals of the pump laser and its background.

Table 1. Wavelengths of Light Associated with the Sum-Frequency Processes.

Peak Number	λ_{SFG} (nm)	λ_{Cal} (nm)	λ_{Meas} (nm)	$\lambda_{Meas} - \lambda_{Cal}$ (nm)
2	769.780	1558.196	1558.416	+0.220
3	770.853	1562.602	1562.463	−0.139
4	772.075	1567.630	1567.545	−0.085
5	775.156	1580.386	1580.290	−0.096
6	775.782	1582.988	1583.006	+0.018
7	776.414	1585.621	1585.675	+0.054
8	777.719	1591.075	1591.075	+0.000
9	779.579	1598.879	1598.763	−0.116

information of the yellow-background highlighted part of Fig. 3(a). We found that the wavelengths λ_{Meas} of the blue peaks in Fig. 3(b) coincide with λ_{Cal} with deviations from 0 nm to 0.220 nm. Accordingly, we attribute the unexpected nonlinear optical signals to the sum-frequency of the pump laser and its background.

Initially, we suspected these nonlinear optical signals may due to the sum-frequency of the pump laser and its third-order nonlinear optical outputs, such as stimulated Raman or four-wave mixing signal. We measured the transmission spectrum around the pump, and neither the Raman nor four-wave mixing signal was observed in the 1550 nm band, especially at the wavelengths that may generate observed nonlinear signals via the sum-frequency process under a 1521.36 nm pump. The absence of the Raman and four-wave mixing signals further verify that the nonlinear optical signals extending from 770 nm to 780 nm are due to the sum-frequency of the laser and its background that was coupled into the LN WGM microcavity. The high power of the background from 1560 nm to 1600 nm makes it easier to generate sum-frequency signals ranging from 770 nm to 780 nm.

The normalized conversion efficiencies of the strongest sum-frequency signal (Peak 7 in Fig. 2) and the associated second harmonic signal were derived by measuring the slope of the curve of the conversion efficiency (P_{signal}/P_{pump}) with respect to the pump power; see Fig. 4. The measured conversion efficiencies of the sum-frequency and SHGs are $6.15 \times 10^{-4}\ \mathrm{mW}^{-1}$ and $4.7 \times 10^{-6}\ \mathrm{mW}^{-1}$, respectively. The efficiency of the SHG is lower than the highest efficiency of second-order nonlinear optical processes related to birefringent phase matching conditions in LN WGM microcavities, which is the order of $0.015\ \mathrm{mW}^{-1}$[27]. The main reason can be described as follows. (1) According to the reference, phase matching in Z-cut single crystal LN microdisk resonators with less than 200 nm thickness and less than 30 μm radius can be achieved in low-order WGMs[34]. In our experiment, the thickness of the disk is not thin enough to achieve frequency conversion between fundamental modes; therefore, we believe high-order modes get involved in the SHG process. The involvement of high-order WGMs in nonlinear optical processes is one of the main reasons that reduce the nonlinear conversion efficiency due to the poor spatial overlap between the WGMs acting in the nonlinear processes. (2) The absence of a broad-band coupling of the tapered fiber with the LN WGM microcavities, which means the lack of efficient coupling in both the 1550 nm and 775 nm bands, results in low nonlinear conversion efficiency as well due to the decreased collecting efficiency of the second-order signals.

It is noted that the SFG process related to the phenomenon itself has meaningful application and has been reported in both millimeter-sized and micrometer-sized LN WGM microcavities[27,35]. High-efficiency SFG can be utilized in a series of applications, such as single photon detection and bioimaging, by converting relatively week signals in the infrared band to the visible band and taking advantage of the high efficiency and low cost of photodetectors in the visible band. On the other hand, the phenomenon observed in our experiment may negatively influence other nonlinear optical effects. (1) The multi-peak signals cause pump energy consumption, reducing other nonlinear optical processes. (2) The sum-frequency between the pump laser and the background leads to nonlinear noise. The higher the pump power is, the more the significant noise is. We could take some methods to avoid these negative influences on nonlinear frequency conversion, such as employing a laser with a high side-mode suppression ratio or applying a band-pass filter to the pump laser.

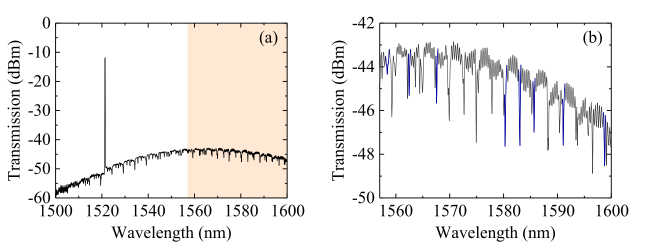

Fig. 3. Transmission spectra of the pump laser and its background. (a) A typical broad transmission spectrum of an LN WGM microcavity coupled to a tapered fiber. (b) The enlarged view of the yellow highlighted part of (a) showing the pump laser background in detail. The peaks marked in blue represent the WGMs associated with the sum-frequency processes.

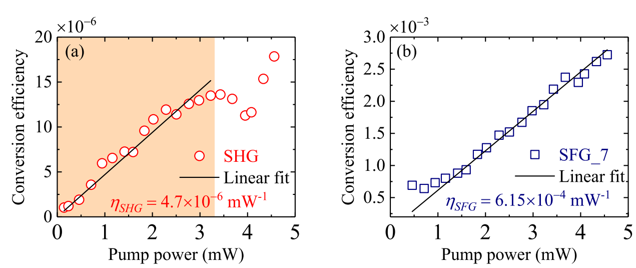

Fig. 4. Dependence of the conversion efficiency of the typical nonlinear optical signals on that of the pump laser. (a) and (b) show the data for the second harmonic signal and that for the sum-frequency signal marked as Peak 7, respectively.

4. Conclusions

To conclude, we observed a series of multi-peak signals in an LN WGM microcavity under the pump of only a continuous laser in the 1550 nm band. These signals were ascribed to the wave mixing of the pump laser and its background, which is usually considered natural light. The influences of SFG between the laser and the background on the nonlinear process were analyzed. The method to suppress the phenomenon was proposed. This work provides a reasonable interpretation for the unknown nonlinear optical signal in WGM microcavities and the suggestions to use and avoid similar phenomena.

Acknowledgement

This work was supported by the National Key Research and Development Program of China (No. 2019YFA0705000), the National Natural Science Foundation of China (Nos. 12034010, 92050111, 12134007, 11734009, 92050114, 12004197, and 12074199), and the Higher Education Discipline Innovation Project (No. B07013).

References

1. Y. Zhi, X. Yu, Q. Gong, L. Yang, and Y. Xiao, "Single nanoparticle detection using optical microcavities," Adv. Mater. **29**, 1604920 (2017).
2. R. Wolf, Y. Jia, S. Bonaus, C. S. Werner, S. J. Herr, I. Breunig, K. Buse, and H. Zappe, "Quasi-phase-matched nonlinear optical frequency conversion in on-chip whispering galleries," Optica **5**, 872 (2018).
3. M. Li, C. Zou, C. Dong, X. Ren, and D. Dai, "Enhancement of second-harmonic generation based on the cascaded second- and third-order nonlinear processes in a multimode optical microcavity," Phys. Rev. A **98**, 013854 (2018).
4. D. Grassani, S. Azzini, M. Liscidini, M. Galli, M. J. Strain, M. Sorel, J. Sipe, and D. Bajoni, "Micrometer-scale integrated silicon source of time-energy entangled photons," Optica **2**, 88 (2015).
5. R. Gao, N. Yao, J. Guan, L. Deng, J. Lin, M. Wang, L. Qiao, W. Fang, and Y. Cheng, "10^8 lithium niobate microring with ultra-high Q factor above," Chin. Opt. Lett. **20**, 011902 (2022).
6. K. Zhang, Z. Chen, H. Feng, W. Wong, E. Y. Pun, and C. Wang, "High-Q lithium niobate microring resonators using lift-off metallic masks," Chin. Opt. Lett. **19**, 060010 (2021).
7. D. Zhu, L. Shao, M. Yu, R. Cheng, B. Desiatov, C. Xin, Y. Hu, J. Holzgrafe, S. Ghosh, and A. Shams-Ansari, "Integrated photonics on thin-film lithium niobate," Adv. Opt. Photonics **13**, 242 (2021).
8. C. Lin, Y. Chen, X. Li, L. Yang, R. Ni, G. Zhao, Y. Zhang, X. Hu, and S. Zhu, "Frequency-doubled vortex beam emitter based on nonlinear Cherenkov radiation," Chin. Opt. Lett. **18**, 071902 (2020).
9. S. Liu, Y. Zheng, and X. Chen, "Cascading second-order nonlinear processes in a lithium niobate-on-insulator microdisk," Opt. Lett. **42**, 3626 (2017).
10. R. Wolf, I. Breunig, H. Zappe, and K. Buse, "Cascaded second-order optical nonlinearities in on-chip micro rings," Opt. Express **25**, 29927 (2017).
11. S. Liu, Y. Zheng, Z. Fang, X. Ye, Y. Cheng, and X. Chen, "Effective four-wave mixing in the lithium niobate on insulator microdisk by cascading quadratic processes," Opt. Lett. **44**, 1456 (2019).
12. G. Lin and Q. Song, "Kerr frequency comb interaction with Raman, Brillouin, and second order nonlinear effects," Laser Photonics Rev. **16**, 2100184 (2022).
13. N. N. David, *Nonlinear Optical Crystals: A Complete Survey* (Springer, 2005).
14. J. Lin, F. Bo, Y. Cheng, and J. Xu, "Advances in on-chip photonic devices based on lithium niobate on insulator," Photonics Res. **8**, 1910 (2020).
15. Y. Kong, F. Bo, W. Wang, D. Zheng, H. Liu, G. Zhang, R. Rupp, and J. Xu, "Recent progress in lithium niobate: optical damage, defect simulation, and on-chip devices," Adv. Mater. **32**, 1806452 (2019).
16. Y. Li, Z. Huang, W. Qiu, J. Dong, H. Guan, and H. Lu, "Recent progress of second harmonic generation based on thin film lithium niobate," Chin. Opt. Lett. **19**, 060012 (2021).
17. J. Lu, J. B. Surya, X. Liu, A. W. Bruch, Z. Gong, Y. Xu, and H. X. Tang, "Periodically poled thin-film lithium niobate microring resonators with a second-harmonic generation efficiency of 250,000%/W," Optica **6**, 1455 (2019).
18. J. Chen, Z. Ma, Y. Sua, Z. Li, C. Tang, and Y. Huang, "Ultra-efficient frequency conversion in quasi-phase-matched lithium niobate microrings," Optica **6**, 1244 (2019).
19. J. Chen, C. Tang, M. Jin, Z. Li, Z. Ma, H. Fan, S. Kumar, Y. M. Sua, and Y. Huang, "Efficient frequency doubling with active stabilization on chip," Laser Photonics Rev. **15**, 2100091 (2021).
20. J. Lin, N. Yao, Z. Hao, J. Zhang, W. Mao, M. Wang, W. Chu, R. Wu, Z. Fang, L. Qiao, W. Fang, F. Bo, and Y. Cheng, "Broadband quasi-phase-matched harmonic generation in an on-chip monocrystalline lithium niobate microdisk resonator," Phys. Rev. Lett. **122**, 173903 (2019).
21. Z. Hao, L. Zhang, W. Mao, A. Gao, X. Gao, F. Gao, F. Bo, G. Zhang, and J. Xu, "Second-harmonic generation using d_{33} in periodically poled lithium niobate microdisk resonators," Photonics Res. **8**, 311 (2020).
22. X. Wu, L. Zhang, Z. Hao, R. Zhang, R. Ma, F. Bo, G. Zhang, and J. Xu, "Broadband second-harmonic generation in step-chirped periodically poled lithium niobate waveguides," Opt. Lett. **47**, 1574 (2022).
23. L. Zhang, Z. Hao, Q. Luo, A. Gao, R. Zhang, C. Yang, F. Gao, F. Bo, G. Zhang, and J. Xu, "Dual-periodically poled lithium niobate microcavities supporting multiple coupled parametric processes," Opt. Lett. **45**, 3353 (2020).
24. Z. Hao, J. Wang, S. Ma, W. Mao, F. Bo, F. Gao, G. Zhang, and J. Xu, "Sum-frequency generation in on-chip lithium niobate microdisk resonators," Photonics Res. **5**, 623 (2017).
25. X. Ye, S. Liu, Y. Chen, Y. Zheng, and X. Chen, "Sum-frequency generation in lithium-niobate-on-insulator microdisk via modal phase matching," Opt. Lett. **45**, 523 (2020).
26. J. Lu, A. Al Sayem, Z. Gong, J. B. Surya, C. Zou, and H. Tang, "Ultralow-threshold thin-film lithium niobate optical parametric oscillator," Optica **8**, 539 (2021).
27. R. Luo, Y. He, H. Liang, M. Li, J. Ling, and Q. Lin, "Optical parametric generation in a lithium niobate microring with modal phase matching," Phys. Rev. Appl. **11**, 034026 (2019).
28. R. Luo, H. Jiang, S. Rogers, H. Liang, Y. He, and Q. Lin, "On-chip second-harmonic generation and broadband parametric down-conversion in a lithium niobate microresonator," Opt. Express **25**, 24531 (2017).
29. J. Lu, M. Li, C. Zou, A. Al Sayem, and H. Tang, "Toward 1% single-photon anharmonicity with periodically poled lithium niobate microring resonators," Optica **7**, 1654 (2020).
30. C. Wang, M. Zhang, M. Yu, R. Zhu, H. Hu, and M. Loncar, "Monolithic lithium niobate photonic circuits for Kerr frequency comb generation and modulation," Nat. Commun. **10**, 978 (2019).
31. D. V. Strekalov, A. S. Kowligy, V. G. Velev, G. S. Kanter, P. Kumar, and Y. Huang, "Phase matching for the optical frequency conversion processes in whispering gallery mode resonators," J. Mod. Opt. **63**, 50 (2016).
32. J. Moore, M. Tomes, T. Carmon, and M. Jarrahi, "Continuous-wave ultraviolet emission through fourth-harmonic generation in a whispering-gallery resonator," Opt. Express **19**, 24139 (2011).
33. J. Moore, M. Tomes, T. Carmon, and M. Jarrahi, "Continuous-wave cascaded-harmonic generation and multi-photon Raman lasing in lithium niobate whispering-gallery resonators," Appl. Phys. Lett. **99**, 221111 (2011).
34. J. Moore, J. K. Douglas, I. W. Frank, T. A. Friedmann, R. M. Camacho, and M. Eichenfield, "Efficient second harmonic generation in lithium niobate on insulator," in *Conference on Lasers and Electro-Optics* (2016), paper STh3P.1.
35. D. V. Strekalov, A. S. Kowligy, Y. Huang, and P. Kumar, "Optical sum-frequency generation in a whispering-gallery-mode resonator," New J. Phys. **16**, 053025 (2014).